Magnetic Properties of Co/Cu/Py Antidot Films With Different Pore Diameters

Juliano C. Denardin[1], Erick Burgos[2], Roberto Lavín[3], Smiljan Vojkovic[3], Joel Briones[1], and Marcos Flores[4]

[1]Departamento de Física, Universidad de Santiago, Santiago 9170124, Chile
[2]Facultad de Ciencias, Universidad de Chile, Santiago 8320000, Chile
[3]Facultad de Ingeniería, Universidad Diego Portales, Santiago 8370191, Chile
[4]Departamento de Física, Universidad de Chile, Santiago 8320000, Chile

The magnetic properties of ordered nanoscale Co/Cu/Py multilayer antidot films with different pore sizes prepared on top of nanoporous alumina membranes (NAMs) are presented. Using Co and Py films separated by a Cu thin layer, and tuning the pore diameters of the NAMs, we were able to play with the coercivity of the films and observe stepped magnetization curves, as a consequence of the different coercivities of the Co and Py films. The magnetic properties of the multilayer antidots have been measured and compared with results obtained for antidots of Cu/Py. The magnetization reversal process that occurs in each individual layer and in the multilayer was studied by means of micromagnetic simulations.

Index Terms— **Magnetic hysteresis, magnetic multilayers, nanoporous materials.**

I. Introduction

NANOSTRUCTURED magnetic elements have received much attention from the scientific community in the last two decades due to their potential applications, ranging from sensors for the electronic and electromechanical industry to the storage media for the magnetic recording industry. The magnetic nanostructures usually referred as antidots are based on magnetic thin films with periodic arrays of holes. In the last years, the study of magnetic nanoparticles based on arrays of antidots have attracted intensive attention because they are a promising candidates for a new generation of ultrahigh-density magnetic storage media, and an exciting topic in fundamental physics [1]–[3]. In an antidot array, magnetic features, such as coercive field, anisotropy axes, and reversal mechanisms, among others, can be tailored by tuning the geometric parameters of the array. In general, the studies have been focused in antidot systems of a single magnetic material. Antidots of Ni–Fe (Py) films are widely studied [3]–[5], presenting an increased coercivity compared with the continuous form. Antidots made of Co present a large enhancement of the coercivity, and are usually deposited with Pt for out of plane recording purposes. Arrays of Co/Cu/Py multilayer antidots, fabricated by UV lithography, have been studied previously [6] and magnetoresistances (MRs) have been used to understand in more detail the magnetization reversal in multilayers [7] and bicomponent antidot nanostructures [8].

In this paper, we present the magnetic properties of ordered nanoscale Co/Cu/Py antidot arrays with different pore sizes prepared on top of nanoporous alumina membranes (NAMs). Using Co and Py films separated by a Cu thin layer, and tuning the pore diameters of the NAMs, we were able to play with the coercivity of the films and observe stepped magnetization curves, as a consequence of the different coercivities of the Co and Py films. By systematic measurements of the magnetic and magnetotransport properties of these samples, and comparing with simulations, we were able to understand in more detail the magnetization reversal that takes place in these multilayer antidots.

Manuscript received March 7, 2014; revised June 11, 2014; accepted June 16, 2014. Date of current version November 18, 2014. Corresponding author: J. C. Denardin (e-mail: jcdenardin@gmail.com).

Color versions of one or more of the figures in this paper are available online at http://ieeexplore.ieee.org.

Digital Object Identifier 10.1109/TMAG.2014.2331973

II. Experimental Procedure

NAMs were prepared from a 0.32 mm thickness aluminum foil (Good-Fellow, 99.999%) using the so-called two-step anodization technique [9]. Prior to the anodization processes, the aluminum foils were cleaned with acetone, isopropanol, and distilled water, and then electropolished for 5–10 min in a CH_3CH_2OH:$HClO_4$ (3:1) solution under 10 V at 4 °C. After this treatment, the samples were submitted to a first anodization, at 40 V for 8 h in a 0.3 M oxalic acid solution at 20 °C. After the first anodization step, the anodized layer was etched with a solution at room temperature during 12 h. This solution is composed of 7 g of H_3PO_4, 1.8 g of H_3CrO_4, and adding H_2O up to complete 100 mL. The ordered pore arrangement was achieved with a 6 h long second anodization step performed under same conditions than the first one. The pore diameter was modified by a posterior treatment in a 5 W% H_3PO_4 solution at 35 °C for 5–10 min producing samples with 40, 50, 65, and 75 nm of pores diameter.

The films were deposited by sputtering on top of NAMs that have been previously anodized in oxalic acid. The thickness of the films was controlled by a crystal balance, and all the samples where sputtered at the same time, having 10 nm of Co, 5 nm of Cu, and 20 nm of Py (NiFe). Another layer with 8 nm of Cu was deposited on top of the films to avoid oxidation.

The magnetic measurements where performed in a home-made alternating gradient magnetometer at room temperature. MR of the samples was measured in a Cryogenic LTD mini 5 T vibrating sample magnetometer (VSM), using the Resistivity probe (RnX) measuring platform.

Micromagnetic simulations were made using the 3-D object-oriented micro magnetic framework (OOMMF) package [10].

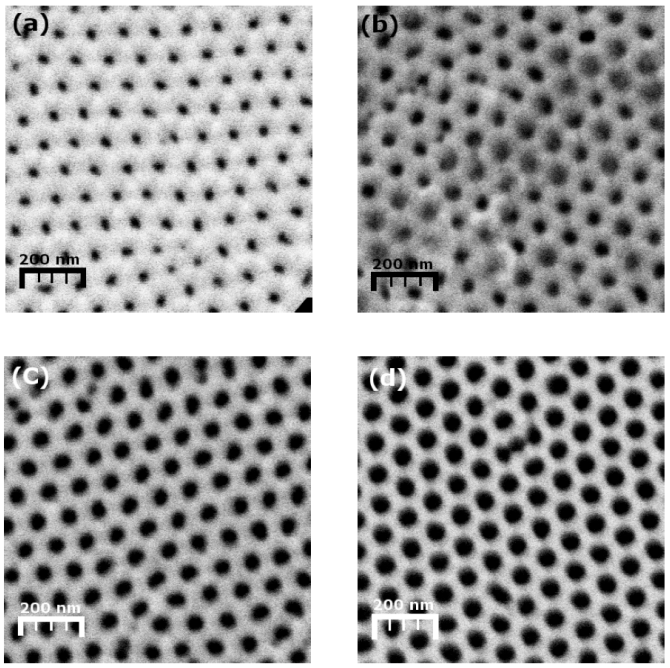

Fig. 1. Co/Cu/Py multilayer films on antidots with pores of different diameters. (a) 40 nm. (b) 50 nm. (c) 65 nm. (d) 75 nm.

The magnetization of the sample is computed as a function of time using damped Landau–Lifshitz–Gilbert equation of motion of the magnetization at zero temperature [11]. Our starting point is a square film of area of 1 μm $\times$ 1 μm and a separation between holes of 100 nm. Thus, the ferromagnetic system is spatially divided into cubic cells of 2 nm $\times$ 2 nm $\times$ 2 nm (smaller than the exchange lengths of materials), and within each cell the magnetization is assumed to be uniform. The micromagnetic simulations are performed using typical Co and Py parameters: saturation magnetization $M_{S,Co} = 1.4\times10^6$ A/m and $M_{S,Py} = 8.6\times10^5$ A/m), exchange stiffness constant $A_{Co} = 3 \times 10^{-11}$ J/m and $A_{Py} = 1.3 \times 10^{-11}$ J/m, and anisotropy constant of $K = 0$ (for polycrystalline films). In all the cases, the damping parameter was chosen as 0.5.

III. Results and Discussion

Fig. 1 shows the SEM images of the Co/Cu/Py films deposited on top of the NAMs. The magnetic films follow the morphology of the patterned membrane, and the area between pores decreases as the pore sizes increases, changing the space available for nucleation and propagation of the domain walls.

Using Co and Py films separated by a Cu thin layer, and tuning the pore diameters of the NAMs, we were able to play with the coercivity of the films and observe stepped magnetization curves, as can be observed in Fig. 2. It was observed that the magnetization reversal of the Co and Py layers occurs at different fields, and the difference in coercivities increases with pore diameter. On the same set of NAMs, we also deposited films of Cu (15 nm)/Py (20 nm). In these films, we observe a small increase in the coercivity with increase of pore diameter, but does not observe the two-step magnetization reversal as in the Co/Cu/Py films [Fig. 2(b)]. In the continuous Co/Cu/Py

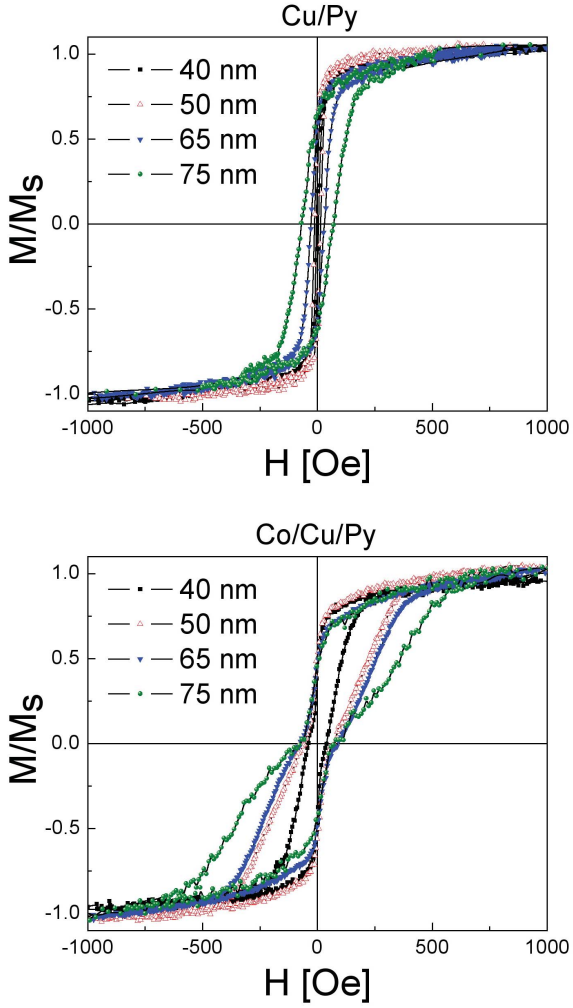

Fig. 2. Magnetization curves of Cu/Py (top) and Co/Cu/Py (bottom) multilayer films on antidots with pores of different diameters.

films, deposited on glass, there is a small two-step effect in the curves, but very small coercivities are observed.

It is worth to note that the magnetization reversal of the Co/Cu/Py multilayer antidots occurs at fields similar to the Cu/Py antidots (their coercivities are comparable). The second step in the hysteresis curve, which appears at a higher field, is the magnetization reversion of the Co layer. Antidots of Co would then have a higher coercivity, which is reduced by the interaction with the Py magnetic layer.

Since the separation among the Co and Py layers is of only 5 nm, magnetostatic and RKKY interactions could be present [12], resulting in a decrease in the coercivity as observed in the experimental curves.

To understand in more detail the magnetization reversal in these multilayers, we have also studied the magnetization reversal process by means of micromagnetic simulations using OOMMF [10]. To perform the micromagnetic simulations, SEM images as from Fig. 1 were treated by image filters and used as masks in OOMMF [4], [5], allowing us reproducing the typical defects observed in the samples.

The thicknesses of the layers in the simulation are 12 nm of Co and 20 nm of Py, separated by a gap of 4 nm. Fig. 3(a)

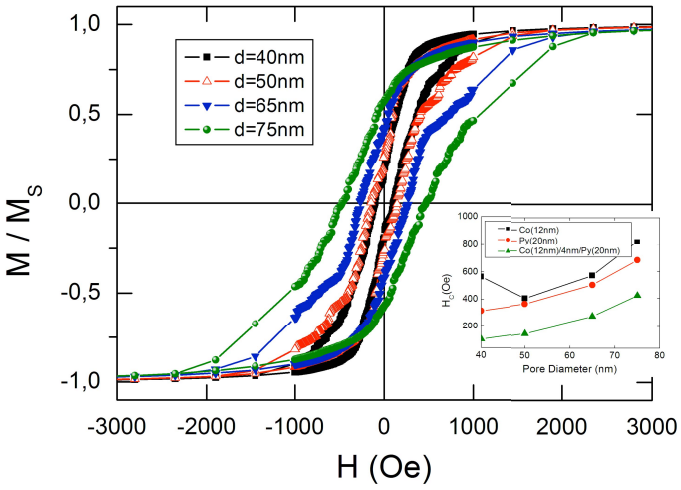

Fig. 3. Simulated magnetization curves for antidots of Co/Cu/Py with different pore diameters and coercivity of the Co, Py, and Co/Cu/Py antidots as function of pore diameter (inset).

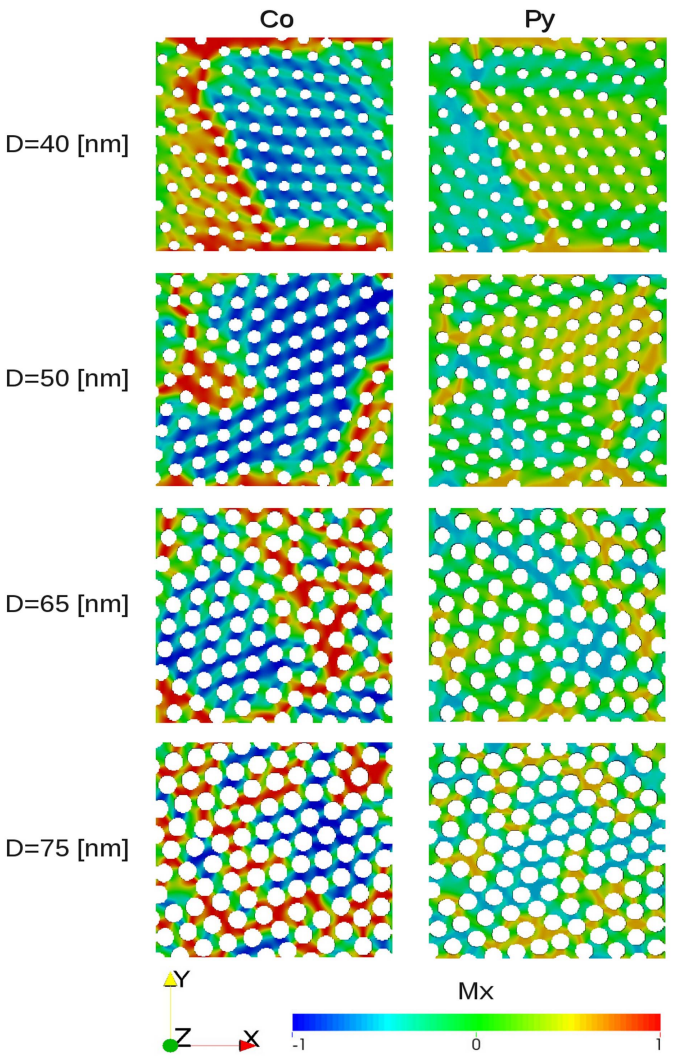

Fig. 4. Simulated images of the magnetization state of Co and Py antidot films with different pore diameters.

shows the simulated hysteresis curves for the Co/gap/Py antidot film (gap is of the same thickness of the Cu layer in the experimental film) in function of the pore diameter, and the inset of Fig. 3 shows the coercivity in function of the pore diameter for the Co/gap/Py antidot film, and antidot isolated films of the Co and Py. The coercivity values of the simulated curves are higher than the observed in the experimental ones, and the steps in the magnetization reversal are not so pronounced as in the experimental curves. Despite the difficulties in reproducing in the simulations all the aspects and complexities of the experimental samples, the results can be useful to observe and understand the domain-wall propagation in the different layers.

Fig. 4 shows the simulated domain configuration in the demagnetized state for different pore diameters for the Co/Gap/Py antidot films. These images are snapshots of the magnetic configuration at $-H_c$ (negative coercivity) state, obtained when the external magnetic field is decreased from $+H_s$ (saturation), and starting with the antidot films saturated in the x-direction. When the size of the pores increases, and the space for the propagation of the domain walls is reduced, the interaction among different propagating domains produces multiple smaller domains and consequently gives rise to a more complex magnetic domain structure, which results in an increase in the coercivity of the films. It is also possible to observe in the images of Fig. 4, the presence of some kind of vortex behavior in the region between some pores. Vortex switching could also be responsible for the reduction of coercivity in the multilayers. In the Co layer, the interactions between different domain walls are stronger than in the Py layer, and the magnetization reversal of the Co layer will occur at larger external fields.

For Co/Gap/Py simulated antidot systems, we obtain a lower coercivity than for antidot systems of a single magnetic material [Fig. 3 (inset)]. This is because the Py antidot film inverts its magnetization at a lower external field than the Co antidot films, and induces the Co film to inverts its magnetization at lower external field, due to the magnetic coupling between both layers. This magnetic coupling is clearly observed in Fig. 4, in the similarity of the magnetic patterns for the Co and Py layers. The magnetostatic interaction favors an antiferromagnetic coupling among the Co and Py layers, being responsible for a loop bifurcation that is also observed in the simulated curves.

Finally, MR measurements have been performed in the samples. Fig. 5 shows the MR curve of the Co/Cu/Py antidot sample with 75 nm pore diameter, measured with the magnetic field transversal to the current configuration. In this graph, the magnetization curve of the same sample is also shown for comparison.

The MR curve shown in Fig. 5 follows the magnetization reversal and does not show the complex peak structure observed by other authors in similar antidot multilayers [6]. The MR response of the sample with the field parallel to the current (longitudinal MR, or LMR) is similar to the one shown in Fig. 5 and does not show anisotropic MR effect. The effect of interlayer exchange coupling in MR curves has been studied

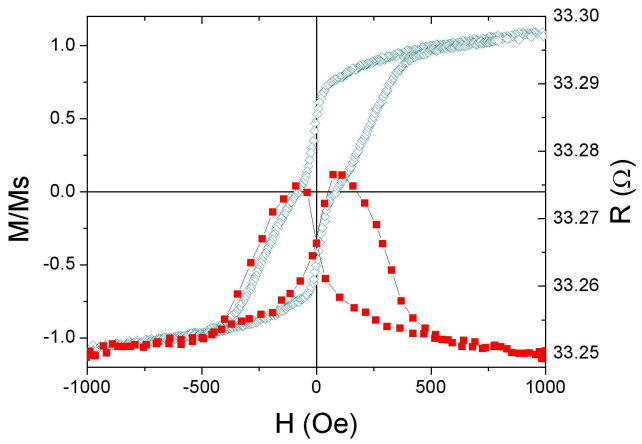

Fig. 5. MR curve of the Co/Cu/Py antidot sample with 75 nm pore diameter (filled red symbols). The magnetization curve of the same sample is also shown for comparison (open green symbols).

previously in Co/Cu/Co continuous films [7], and complex MR curves have been observed when the Cu thickness was 5 nm, corresponding to an antiferromagnetic coupling among the layers.

In antidots fabricated by anodization process, the roughness of the AAO topography is of the order of 10 nm [13], and plays an important role in the magnetotransport properties.

It is known that the interlayer exchange coupling strongly dependent of the interlayer roughness, being the roughness responsible for the appearance of dipolar interaction between the layers [12]. The isotropic MR response that is observed in these AAO antidots could be consequence of the topography of the samples.

IV. Conclusion

By systematic measurements of the magnetic properties of Co/Cu/Py and Cu/Py multilayer antidots, and comparing the results with simulations, we were able to understand in more detail the magnetization reversal that takes place in these systems. The Co/Cu/Py antidots present hysteresis curves with two steps that correspond to the magnetization reversal of the Py and Co layers. The progressive increase in the distribution of coercivities and interactions gives rise to more complex magnetic domain structures when the diameter of the pores increase, which results in an increasing in the coercivity of the films. On the other hand, the interaction between different magnetic layers decreases the coercivity of the multilayer films.

Acknowledgment

This work was supported in part by Fondecyt under Grants 1140195, 3120059, and 11110130; in part by the Project Millennium Science Nucleus in Basic and Applied Magnetism under Grant N°P10-061-F; in part by Anillo ACT1117; and in part by CONICYT BASAL CEDENNA FB0807.

References

[1] R. P. Cowburn, A. O. Adeyeye, and J. A. C. Bland, "Magnetic domain formation in lithographically defined antidot permalloy arrays," *Appl. Phys. Lett.*, vol. 70, no. 17, p. 2309, 1997.

[2] L. Torres, L. Lopez-Diaz, and J. Iñiguez, "Micromagnetic tailoring of periodic antidot permalloy arrays for high density storage," *Appl. Phys. Lett.*, vol. 73, no. 25, p. 3766, 1998.

[3] M. T. Rahman, N. N. Shams, and C.-H. Lai, "A large-area mesoporous array of magnetic nanostructure with perpendicular anisotropy integrated on Si wafers," *Nanotechnol.*, vol. 19, no. 32, p. 325302, 2008.

[4] J. L. Palma *et al.*, "Magnetic properties of Fe_{20} Ni_{80} antidots: Pore size and array disorder," *J. Magn. Magn. Mater.*, vol. 344, pp. 8–13, Oct. 2013.

[5] R. L. Rodríguez-Suárez *et al.*, "Ferromagnetic resonance investigation in permalloy magnetic antidot arrays on alumina nanoporous membranes," *J. Magn. Magn. Mater.*, vol. 350, pp. 88–93, Jan. 2014.

[6] C. C. Wang, A. O. Adeyeye, and N. Singh, "Magnetic and transport properties of multilayer nanoscale antidot arrays," *Appl. Phys. Lett.*, vol. 88, no. 22, p. 222506, 2006.

[7] A. O. Adeyeye, M. T. Win, T. A. Tan, G. S. Chong, V. Ng, and T. S. Low, "Planar Hall effect and magnetoresistance in Co/Cu multilayer films," *Sens. Actuators A, Phys.*, vol. 116, no. 1, pp. 95–102, 2004.

[8] D. Tripathy, P. Vavassori, J. M. Porro, A. O. Adeyeye, and N. Singh, "Magnetization reversal and anisotropic magnetoresistance behavior in bicomponent antidot nanostructures," *Appl. Phys. Lett.*, vol. 97, no. 4, p. 042512, 2010.

[9] H. Masuda and K. Fukuda, "Ordered metal nanohole arrays made by a two-step replication of honeycomb structures of anodic alumina," *Science*, vol. 268, no. 5216, pp. 1466–1468, 1995.

[10] M. K. Donahue and D. G. Porter. (2002). *OOMMF User's Guide Version 1.2a3*. [Online]. Available: http://math.nist.gov/oommf

[11] T. L. Gilbert, "A phenomenological theory of damping in ferromagnetic materials," *IEEE Trans. Magn.*, vol. 40 no. 6, pp. 3443–3449, Nov. 2004.

[12] D. Altbir, M. Kiwi, R. Ramirez, and I. K. Schuller, "Dipolar interaction and its interplay with interface roughness," *J. Magn. Magn. Mater.*, vol. 149, no. 3, pp. L246–L250, 1995.

[13] D. C. Leitao *et al.*, "Tailoring the physical properties of thin nanohole arrays grown on flat anodic aluminum oxide templates," *Nanotechnol.*, vol. 23, no. 42, p. 425701, 2012.